

Experimental Analysis of Nanofluids in PEMFC Cooling Plate Integrated with Thermoelectric Generator

A.A. Zailan, I.A. Zakaria*, A.N. Zarizi

School of Mechanical, College of Engineering,

Universiti Teknologi MARA, 40450 Shah Alam, Selangor, MALAYSIA

*irnieazlin@uitm.edu.my

ABSTRACT

A thermoelectric generator (TEG) is considered a feasible option to recover waste heat from a Proton exchange membrane fuel cell (PEMFC) into electrical energy. However, its application is limited due to its low efficiency. Meanwhile, nanofluids have emerged as an alternative coolant in heat transfer due to their superior thermal conductivity characteristics. Thus, this study aims to improve the efficiency of the TEG using nanofluids. The experimental study was conducted on a test bench that coupled a PEMFC cooling plate and TEG which was subjected to a 0.5% volume concentration of $Al_2O_3 : SiO_2$ hybrid nanofluids at a flow rate of Re 300 to 1000. The mixture ratio of $Al_2O_3 : SiO_2$ hybrid nanofluids studied was 10:90 ratio, single nanofluids of Al_2O_3 and SiO_2 and also the base fluid of water. Upon completion, the improvement in power output due to an improved temperature difference of the thermoelectric generator (TEG) is observed. The highest TEG performance was shown by hybrid nanofluids of 10:90 ($Al_2O_3 : SiO_2$) with a 17% improvement as compared to the base fluid of water. This is due to the bigger temperature difference which is caused by better thermal conductivity of hybrid nanofluids as compared to the base fluid.

Keywords: Thermoelectric Generator (TEG); Nanofluids; Aluminium Oxide; Silicone Oxide; Proton Exchange Membrane Fuel Cell (PEMFC)

Introduction

Recently, Proton Exchange Membrane Fuel Cells (PEMFCs) have gained a lot of interest in the transport sector and portable applications because of their high efficiency and low emissions. PEMFCs utilize a polymer electrolyte membrane which sits between the anode and cathode catalyst, to permit protons to move from anode to cathode while preventing the electrode from doing the same cycle. PEMFC converts chemical energy that is released during the electrochemical reaction of hydrogen and oxygen into electrical energy. Their characteristics are operating in low temperatures between 60 °C to 80 °C, having a high-power density as well as ease of make-up, thus, this makes PEMFCs a favourable option for future production of power [1]. However, PEMFC's practical efficiency ranges between 45 to 65% and its thermodynamic limit is 80% [2]. So, an effective heat and thermal management of PEMFC is needed for high energy efficiency and durability of the device. Technology can remain sustainable and become more economical by increasing energy efficiency. Waste Heat Recovery (WHR) has appeared to be effective in increasing the PEMFC's energy efficiency as well as cutting its operational costs while lowering Greenhouse Gases (GHGs) emissions [3]. WHR refers to using heat loss within the system as opposed to releasing it into the environment where it can be used to generate more heat, electricity, or mechanical power for specific purposes [4]. However, since PEMFC optimum operating temperature is low, the temperature difference between the ambient is small. This makes the waste heat recover low in grade. Due to that, there are not many studies about the waste heat recovered in PEMFC.

Additionally, there are a variety of heat recovery devices available to capture the waste heat and among all methods, Thermoelectric Generators (TEGs) have been considered as the most favourable method. Alam et al. [5] study that a thermally coupled TEG and Metal Hydride (MH) cylinder can efficiently be used for waste heat recovery from PEMFC compared to cooling the cold side of TEG naturally or using an external fan. The result shows that heat dissipation from PEMFC increases significantly with TEG power output with a maximum temperature difference of 3.2 °C Generally, a TEG is a device that utilizes the Seebeck effect of semiconductor materials where they are capable of directly converting heat into electricity. The TEG's main elements consist of a Heat Exchanger (HEX), Thermoelectric Modules (TEMs), and a heat sink. It operates to produce electricity when there is a temperature difference between the hot side and the cold side of the generators [6]. The higher temperature difference is advantageous to create power generations that can be obtained by reducing the cross-sectional areas of the conductors and increasing the thicknesses. However, too much temperature difference across the TEG module will make the materials cannot sustain, so, TEG should be operating optimally within the feasible temperature range to reach material stability [7]. TEGs have matchless advantages, where they are environmentally

safe, have no economy-scale-of effect, and operate quietly as they can generate electricity without using mechanical mechanisms or rotating elements [6]. Therefore, TEGs are being used in various applications such as solar energy operation and automobile exhaust waste heat recovery [8].

Nevertheless, despite being used in various applications, TEG is still not widely commercialized because of its low efficiency as a thermoelectric material. The efficiency of TEG depends on the temperature difference between the cold and hot sides of the TEG. In some applications, the temperature of the heat source is fixed. Thus, some studies focus on enhancing its efficiency. According to Meng et al. [9], the system performance of TEG can significantly elevate effectively if the heat transfer coefficient of the system's cold side is enhanced. Furthermore, studies by Ramkumar et al. [10], show the temperature gradient between the hot side and the cold side of TEG is increased when the cooling side droops with thermacool 0.3M coating, which subsequently increases the performance of the device. In addition, Karthick [11] discussed that solar thermal system configurations could increase the efficiency of TEG depending on a given thermoelectric material through optical concentrators that provide a high emissive power density and are able to create a large temperature difference. Due to low efficiency, TEG is only able to convert a small portion of heat energy into electric energy. Theoretically, the dimensionless figure of merit, ZT value is the merit coefficient that evaluates thermoelectric efficiency. A higher ZT value will enhance the conversion efficiency η and the coefficient of performance, COP value of TEG systems, which further enhances the output power. Therefore, the performance of energy conversion of TEG can be enhanced with the help of nanofluids as coolant since nanofluids are known to have higher thermal conductivity [12].

Thermal conductivity is the key in convective heat transfer fluids as lower thermal conductivity will restrict cooling and heating performance. Ruan [12] studies that the nanofluid properties have a significant effect on the performance enhancement of thermoelectrical systems which enlarges the temperature difference in the TEG system, either by increasing the nanoparticle weight concentration or the flow rate of the fluids. Nanofluids have been suggested by researchers recently as a replacement for existing heat transfer fluids. Nanofluid refers to a fluid that contains particles with dimensions less than 100 nm and the types of nanofluid that are commonly used are metal, metal oxide, carbon nanotubes, and carbides. While the base fluid for the nanoparticle to disperse can be aqueous or non-aqueous in nature where typically used are water, ethylene glycol, and oil [13]. Based on the Sezer et al. [13] studies, the highest thermal conductivity enhancement reported is 100% for Multi-Walled Carbon Nanotubes (MWCNTs) nanofluid compared to 65% for Au nanofluids and more than 100% enhancement was reached when magnetic nanoparticle dispersed in different types of base fluids. Even so, long-term stability is the first basic requirement in nanofluids

research for maintaining their enhanced thermophysical properties [13]. Next, Khedkar [14] reported that 5% of Copper Oxide (CuO) nanoparticles concentration with water and ethylene glycol nanofluids has enhanced 23% of thermal conductivity compared to pure base fluids. A higher concentration of particles could enhance the thermal conductivity of nanofluids. However, high viscosity in nanofluids will require a high pumping power which causes a limited use of nanofluids in industrial applications [15].

In the latest advances in the applications of thermoelectric generators reviewed by He et al. [16], none of the TEG applications hybridize with nanofluids application as of today which serves as the research gap that motivates this study. The TEG hybridize with nanofluids has been explored in photovoltaic (PV) cell cooling by Abdelkareem et al. [17] which investigated the effect of Aluminum Oxide (Al_2O_3), Copper Oxide (CuO), Iron Oxide (Fe_3O_4), and Silicone Oxide (SiO_2) nanofluids were used as coolants for TEG. Apart from solar PV cooling, TEG-nanofluids also have been investigated in automotive applications as performed by Karana and Sahoo [18] who use Magnesium Oxide (MgO) and Zinc Oxide (ZnO) nanofluid coolants in their theoretical analysis. They later experimented with automobile waste heat recovery systems with EG-water (EG-W) mixture, ZnO, and SiO_2 nanofluid as coolants for the TEG system [19]. The performance of Graphene Nanoplatelets (GNPs) nanofluids in heat exchangers has also been explored by Ruan et al. [12] who proved that the application of nanofluids is able to boost the cooling capability for TEGs and thermoelectric coolers (TECs).

In this study, an experimental study was performed on the test bench to observe the effect of the difference in cooling fluids on the heat transfer performance of the PEMFC cooling plate in terms of waste heat recovery performance from PEMFC. The studied working fluid was 0.5% concentration of $Al_2O_3 - SiO_2$ with base fluid of distilled water volume ratio of 10:90. The performance of the heat transfer of hybrid nanofluids was compared against mono nanofluids of Al_2O_3 , SiO_2 , and also the base fluid of water. At the end of the study, the performance of TEG with all cooling fluids at 80 °C operating temperature was reported.

Methodology

Nanofluid preparation

This study used an Aluminum Oxide (Al_2O_3) nanoparticles purity in powder form that was purchased from Sigma-Aldrich with 13 nm in size. Meanwhile, Silicone oxide (SiO_2) is in liquid form and is 30 nm in size. Table 1 lists the thermos-physical properties of the nanoparticles and nanofluids employed. The two-step method was employed in this study instead of the one-step method because it is simpler and more convenient given that processed nanoparticles are readily available in the market.

Table 1: Thermo-physical properties of nanoparticles and fluids

Property	Al_2O_3	SiO_2	Distilled water
Density, ρ (kg/m^3)	4000	2220	996
Thermal conductivity, k (W/m.K)	36	1.4	0.615
Specific heat, C_p (J/kg.K)	765	745	4178
References	[16], [17]	[16], [17]	[16], [17]

The Al_2O_3 and SiO_2 single nanofluids were initially prepared separately with the base fluid of distilled water. The Al_2O_3 powder was dissolved in the distilled water, while the liquid form of SiO_2 was diluted to attain a 0.5% volume concentration [20]. Once completed, the nanoparticles underwent a mixing process to ensure the nanoparticles were mixed evenly, where they were mixed physically for 15 minutes using an electric stirrer as shown in Figure 1. Then, the mixed nanoparticles were put in the ultrasonic homogenizer for 120 minutes. This is to ensure the nanofluids become more stabilized as Hong et al. [6] found a reduction in the aggregated size of the nanoparticles with the increase in sonication time, which resulted in the higher stability of the nanofluids.



Figure 1: (a) Mixing process, (b) sonicating process

After the preparation of single nanofluids was completed, a mixture ratio of the 10:90 hybrid nanofluids $Al_2O_3 - SiO_2$ was then prepared. Both single and hybrid nanofluids were prepared using the following formulations.

The conversion of mass concentration into volume concentration:

$$\phi = \frac{\frac{m_p}{\rho_p}}{\frac{m_p}{\rho_p} + \frac{m_{bf}}{\rho_{bf}}} \times 100 \quad (1)$$

where m_p is the mass concentration of the nanoparticles given by the supplier, and ρ is the density in kgm^{-3} , with subscript p and bf representing nanoparticle and base fluid, respectively.

Equation of nanofluids dilution:

$$\Delta V = (V_2 - V_1) = V_1 \left(\frac{\phi_1}{\phi_2} - 1 \right) \quad (2)$$

where ΔV is the volume of water required to be added into the current base fluid, V_1 with the concentration volume of ϕ_1 to obtain the nanofluids volume V_2 and the nanofluids volume concentration of ϕ_2 [20].

The density of the nanofluid can be calculated by using the equation :

$$\rho_{n_f} = \phi \rho_p + (1 - \phi) \rho_{bf} \quad (3)$$

The specific heat of nanofluid is determined by:

$$C_{n_f} = \frac{(1 - \phi)(\rho c)_{bf} + \phi (\rho c)_p}{(1 - \phi)\rho_{bf} + \phi \rho_p} \quad (4)$$

Viscosity is computed using the equation:

$$\mu_{n_f} = \frac{1}{(1 - \phi)^{2.5}} \mu_{bf} \quad (5)$$

The hydraulic diameter, D_h is calculated using the equation, where $a = 5$ cm and $b = 1$ cm:

$$D_h = \frac{4ab}{2(a + b)} \quad (6)$$

The Reynold number (Re) for the experiment is determined by using the equation:

$$Re = \frac{D_h V_{m_p}}{\mu} \quad (7)$$

The volume flow rate can be calculated using the equation:

$$\dot{v} = v_m A_c \quad (8)$$

The mass flow rate can be calculated by using the equation:

$$\dot{m} = \rho_{nf} V_m A_c \quad (9)$$

Thermal conductivity of nanofluid

The thermal conductivity values of nanofluids at a working temperature of 60 °C were referred from the experimental values studied by Khalid et al. [20] as shown in Figure 2. The study found that the hybrid $Al_2O_3 - SiO_2$ nanofluids have better enhancement of thermal conductivity as compared to the based fluid where the highest value of thermal conductivity recorded was with hybrid nanofluids with a volume ratio of 10:90 ($Al_2O_3 - SiO_2$) with the value of 1.018 W/m K or 51.9% enhancement as compared to the base fluid. The study also highlighted that the higher the Al_2O_3 content, the lower the value of thermal conductivity. Thus, for the improvement of the heat transfer in PEMFC, the hybrid nanofluids of $Al_2O_3 : SiO_2$ with a lower ratio of Al_2O_3 are much preferred as it enhances the thermal conductivity property of the base fluid as compared to single nanofluid.

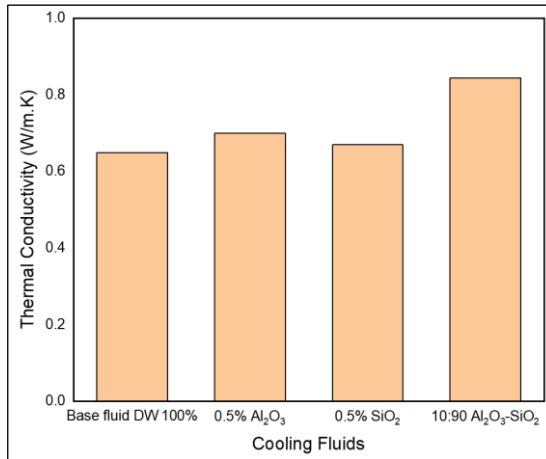


Figure 2: Thermal conductivity of various nanofluids studied [16]

Thermoelectric generation specification thermal conductivity of nanofluid

In this study, TEG devices model SP1848-27145 made from Bismuth Telluride with a dimension of 40 x 40 x 3.4 mm were used. Nine identical TEGs were

attached between the serpentine cooling plate and the heater pad. The TEGs were connected in series into a DC electric load. The hot side of the TEG was attached to the upper side of the heater pad where the heater pad replicates the hot surface temperature of PEMFC. The TEG will absorb the heat dissipate which increases the temperature of hot sides of the TEGs. Meanwhile, the cold side of the TEG was attached to the backside of the serpentine cooling plate. The effect of nanofluids flowing on the serpentine cooling plate will affect the temperature difference of the TEG.

In addition to this, eight k-type thermocouple sensors were utilized to record the temperature in this experiment. The first sensor was placed on the inlet while the second sensor was located on the outlet of fluid flow through in the set-up experiment. The rest of the sensors were attached on the hot side and the cold side of the TEG at positions 1, 2, and 3, respectively as illustrated in Figure 3.

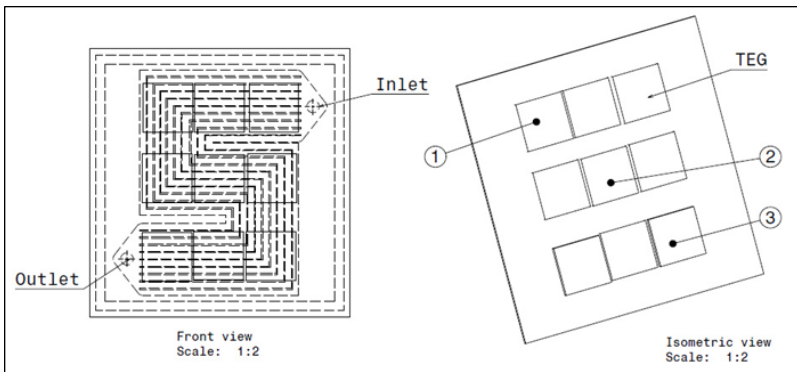


Figure 3: TEG arrangement

Experimental setup

A test bench is established as illustrated in Figure 4 to simulate PEMFC operating conditions with variable flow rate, resistance, and temperature. The PEMFC cooling plate assembly details are shown in Figure 5. The TEG is connected to a DC electric load that could provide resistance from 0Ω to 900Ω as well as measured voltage and ampere of the TEG. The serpentine cooling plate used is made from stainless steel to mimic the lightweight material of the cooling plate in the PEMFC and is $220 \times 210 \times 2.5$ mm in dimension. As for the heating element, a Keenovo silicone heater pad with a heating output of 100 W is set at $80 \text{ }^\circ\text{C}$ for the TEG hot side during the experiment to replicate the surface temperature of PEMFC.

Furthermore, a water pump is utilized for the $\text{Al}_2\text{O}_3 - \text{SiO}_2$ nanofluids coolant to flow through the cooling plate ranging from 100 Re to 600 Re which measured using flowrate meter. At the same time, the heated nanofluids are

cooled down through the radiator before the nanofluids are recirculated back to the coolant tank's storage. The temperature profile of the TEG, inlet, and outlet of the plate is recorded using a GL220 data logger. The schematic diagram of the experimental test bench is illustrated in Figure 6.

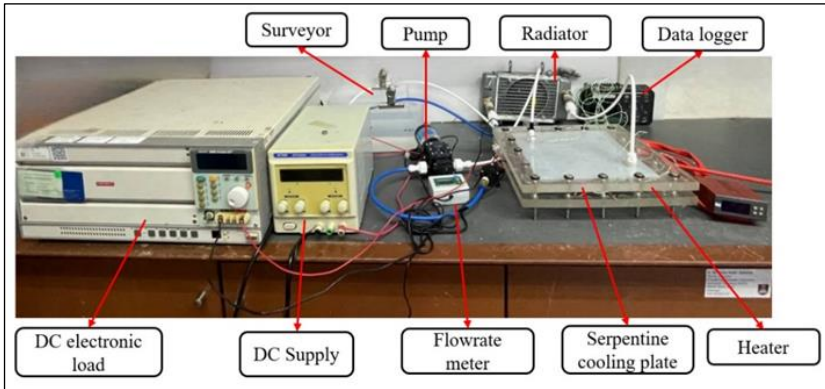


Figure 4: Experimental test bench

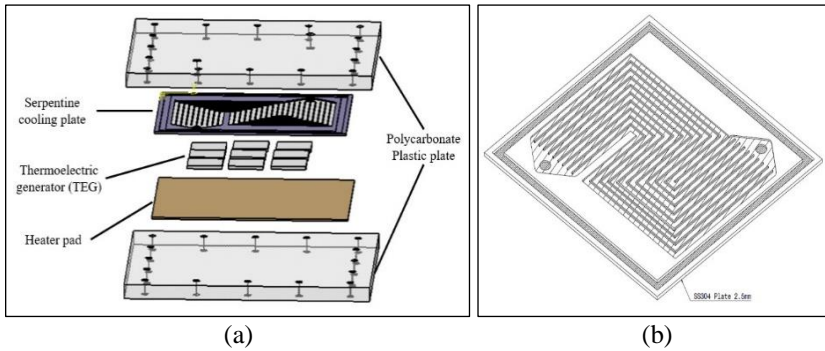


Figure 5: (a) PEMFC-TEG set-up assembly and (b) isometric view of serpentine cooling plate

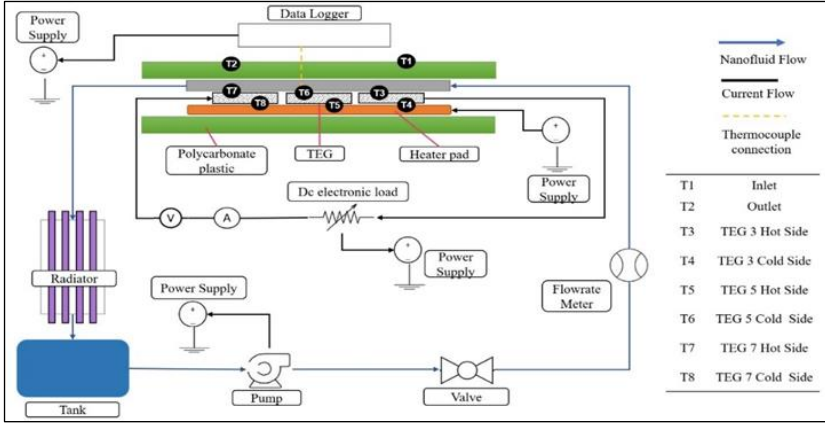


Figure 6: Schematic diagram of the experimental set-up

Mathematical model

To calculate the rate of heat transfer :

$$\dot{Q} = \dot{m}c_{\rho n f} (T_{out} - T_{in}) \quad (10)$$

To obtain the value of heat flux, q, Wm^{-2} :

$$q = \frac{Q}{2(a + b)c} \quad (11)$$

The convective heat transfer coefficient, $WK^{-1}m^{-2}$, can be obtained from equation:

$$h = \frac{q}{A_c(T_{avg} - T_{\infty})} \quad (12)$$

T_{avg} is calculated using :

$$T_{avg} = \frac{\sum T_{surface}}{5} \quad (13)$$

T_{∞} is calculated using equation:

$$T_{\infty} = \frac{T_{in} + T_{out}}{2} \quad (14)$$

The Nusselt number is determined by using equation:

$$Nu = \frac{h}{k} D_h \quad (15)$$

Results and Discussion

Stability analysis

The stability of the single Al_2O_3 , single SiO_2 , and hybrid nanofluids of $Al_2O_3 - SiO_2$ dispersed in distilled water were measured using the visual observation method. The nanofluids samples prepared were evaluated for visual sedimentation after a week and two months after preparation. Figure 7 illustrates the prepared samples right after the preparation and after two months of preparation. It was observed that there was almost negligible sedimentation or coagulation in all samples prepared except for the single Al_2O_3 and hybrid nanofluids of $Al_2O_3 - SiO_2$ as a trace of sedimentation was visible in the sample. However, the sedimentation is not a big concern since the nanofluids will flow through forced convection using a pump. The stability of the nanofluids is important to ensure that the prepared samples is stable before being experimented. Better stability also resembles better dispersion of nanofluids, which will improve the thermal conductivity of the nanofluids [21].

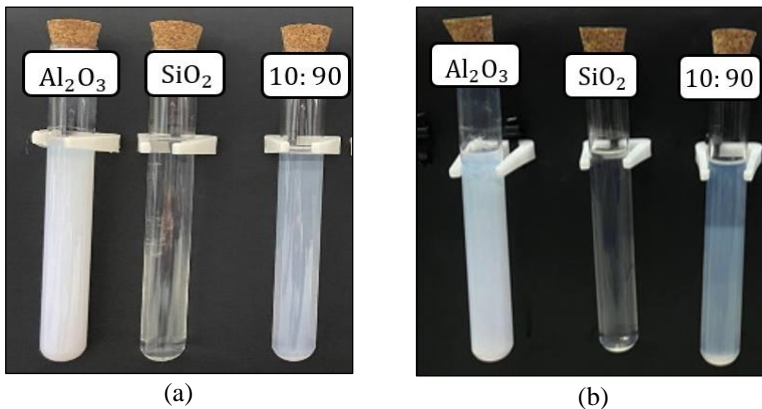


Figure 7: (a) Nanofluids after preparation (b) nanofluids after two months of preparation

Heat Transfer Performance

In this study, the nanofluids were employed as coolants, and the heat transfer performance of the TEG at a working temperature of 80 °C was observed.

Figure 8 shows the average temperature profile of the cooling plate against the Re . It was observed that the average temperature decreased as the Re increased. The average temperature of the cooling plate for all fluids was colder at Re 600 as compared to lower Re . This was due to the effect of the fluid's dynamic as the flow rate was increased. Higher fluid dynamics resulted in lower average temperatures. The result also shows that the hottest temperature was recorded by distilled water. Meanwhile, the temperature profile was reduced gradually when using nanofluids as compared to distilled water. The lowest average temperature was recorded by the hybrid nanofluids at 10:90 with a 17% reduction as compared to distilled water. In addition, the average plate temperature of a single Al_2O_3 and single SiO_2 nanofluids were also significantly improved with 12% and 6% reduction respectively as compared to distilled water plate temperature. This pattern was well-agreed with the thermal conductivity hierarchy of nanofluids studied. Khalid et al. [20] reported that the hybrid nanofluids of $Al_2O_3 - SiO_2$ (10:90) has the highest thermal conductivity value among all nanofluids studied, followed by single Al_2O_3 and single SiO_2 nanofluids, and finally distilled water. The result proved that hybrid nanofluids have the highest capability to improve the heat transfer performance as compared to the base fluid. Higher heat transfer surface between the particles and fluids has enabled the nanofluids to disperse well and eventually transfer the heat more effectively. The hybrid nanofluids that combine both 13 nm Al_2O_3 and 30 nm SiO_2 provides additional contact surface, thus improving the heat transfer [22].

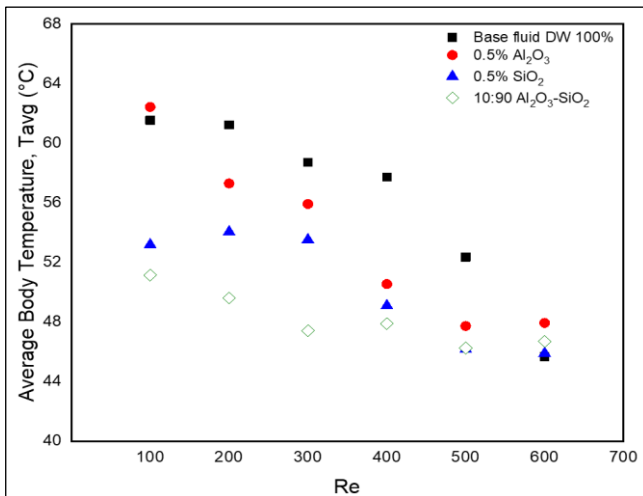


Figure 8: Average temperature profile of the cooling plate against Re

The heat transfer coefficient against Re is illustrated in Figure 9. The mixture ratio of 10:90 hybrid nanofluids showed the highest heat transfer coefficient with 66.03% higher as compared to base fluid followed by single Al_2O_3 and single SiO_2 with 15.18% and 55.11%, respectively. It was also observed that the heat transfer coefficient was increased as the value of Re increased. This was due to the higher flow rate employed at higher Re helped to disperse the heat better than in lower flow rate. The heat transfer coefficient of hybrid nanofluids was higher than the base fluid and single nanofluids due to the dynamic behaviour of nanoparticles suspended in the base fluid which is termed as Brownian motion. The Brownian motion is a random movement of particles that will enhance the viscosity and thermal conductivity of the nanofluids [23].

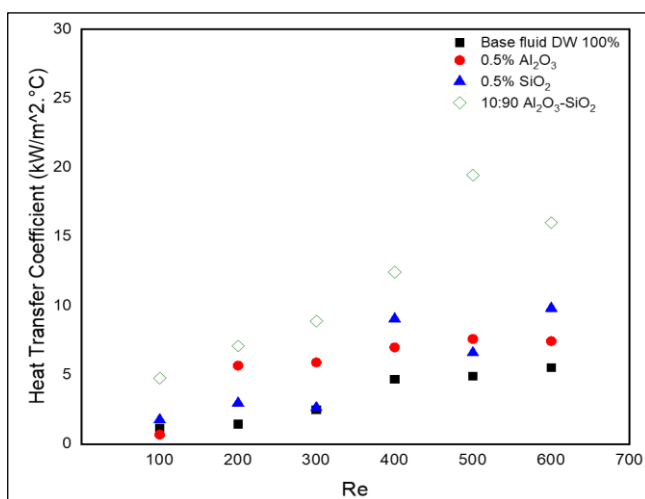


Figure 9: Heat transfer coefficient against Re

A dimensionless Nusselt number can be described as the ratio of thermal energy convected to the fluid with the thermal conducted within the fluid. The higher value of the Nusselt number has better effectiveness of convection heat transfer. Figure 10 shows the Nusselt number against the Re and it is linearly related to the Re . A higher Re will result in a higher Nusselt number. It was observed that 10:90 hybrid nanofluids showed a 3.8 times higher Nusselt number at Re 500 as compared to the base fluid of distilled water. This was then followed by a single Al_2O_3 , single SiO_2 with 1.5 times and 1.3 times higher than the base fluid. Higher Nusselt indicates that the convective heat transfer effect was more dominant than the conductive heat transfer to these nanofluids.

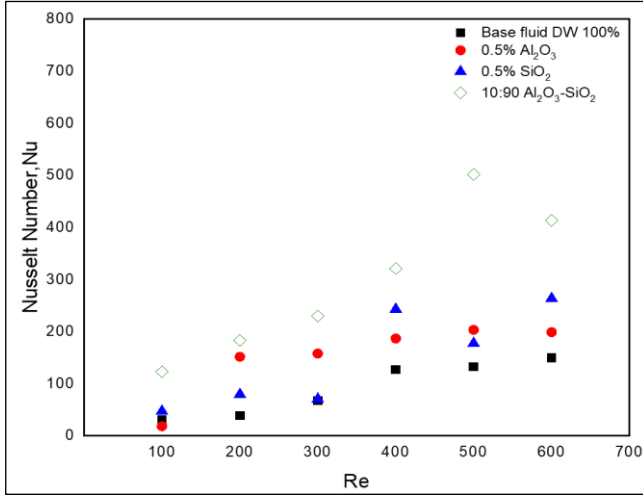


Figure 10: Nusselt number against the Re

Thermoelectric Generator (TEG) performances

TEG performance for distilled water

Figure 11 illustrates the relationship between the current and voltage obtained for all flow rates for the base fluid of distilled water with a resistance range of 0 to 900 Ω . These parameters will determine the power output from the TEG. The results showed that the higher the flow rates, the higher the power obtained. A similar pattern was also highlighted by Raihan et al. [24] who concluded that as the flow rate increased, the TEG power output also increased. Based on Figure 12, the highest power output was obtained at 21.9 ml/s with 26.9 mW, which is equivalent to 2.5 times higher than the lowest flow rate studied at 3.7 ml/s. It was then followed by 18.3 ml/s with 2.3 times higher and then 14.6 ml/s with 2.2 times improved than the lowest flow rate. The improvement was due to the higher temperature difference recorded as the flow rate was increased. The higher flow rate will result in a lower cold side of TEG thus increasing the temperature difference and performance output eventually.

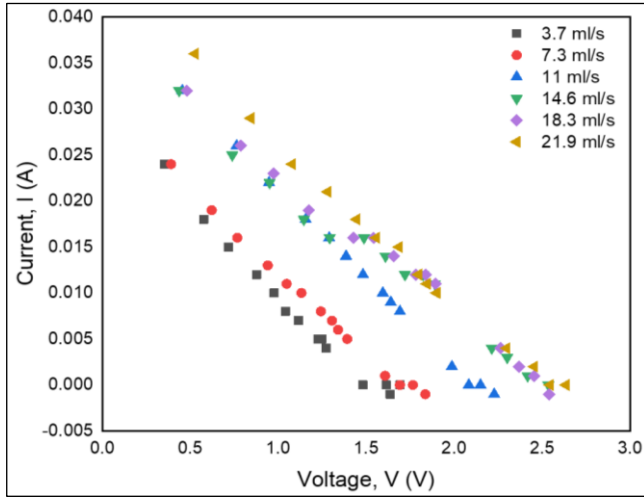


Figure 11: Current, A against Voltage, V for based fluid distilled water

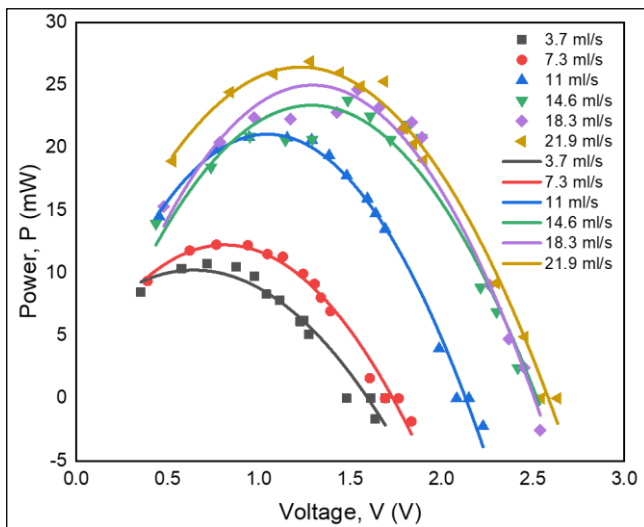


Figure 12: Power, *mW* against Voltage, V for based fluid distilled water

TEG performance for nanofluids

The power output of a TEG is the result of the temperature difference between the cold and hot sides of the TEG. The hybrid nanofluids of 10:90 ratio gave the highest temperature difference between the hot and cold sides of TEG. This

is due to the highest rank in thermal conductivity properties among the types of nanofluids studied as reported by Khalid et al. [20]. The hierarchy of TEG performance matched the hierarchy of thermal conductivity of the nanofluids studied which was reported to be highest in hybrid nanofluids at 10:90, followed by single Al_2O_3 , single SiO_2 , and finally distilled water. Higher value of thermal conductivity has resulted a higher Brownian motion in the nanofluids which has increased the heat transfer effect as shown in Figure 13. The figure displays the variation in current against voltage for all nanofluids studied which were single Al_2O_3 , single SiO_2 , and hybrid nanofluids of $Al_2O_3 - SiO_2$ 10:90 when compared against distilled water in term of the TEG performance at the highest flow rate of Re 600. Reynold number, Re is used in this comparison instead of flow rate (ml/s) as it is a dimensionless number in which the effect of viscosity is considered in determining the velocities of different fluids studied. In Figure 14, the highest power output was observed in hybrid nanofluids of 10:90 with 35.6% higher than the base fluid of distilled water. This was then followed by the single Al_2O_3 nanofluids with 32.7% improvement. The single SiO_2 nanofluids also has improved the TEG performance with 19.4 % enhancement as compared to distilled water. Thus, it was shown that the application of nanofluids can increase the temperature difference of the TEG, therefore improving its performance by obtaining higher power output.

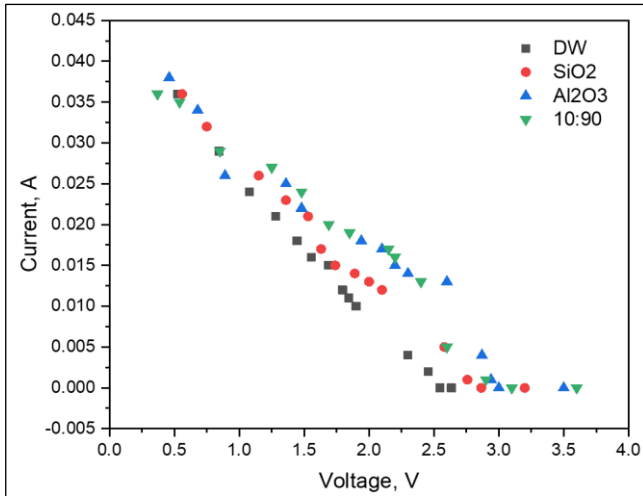


Figure 13: Current, A against Voltage, V for all fluids

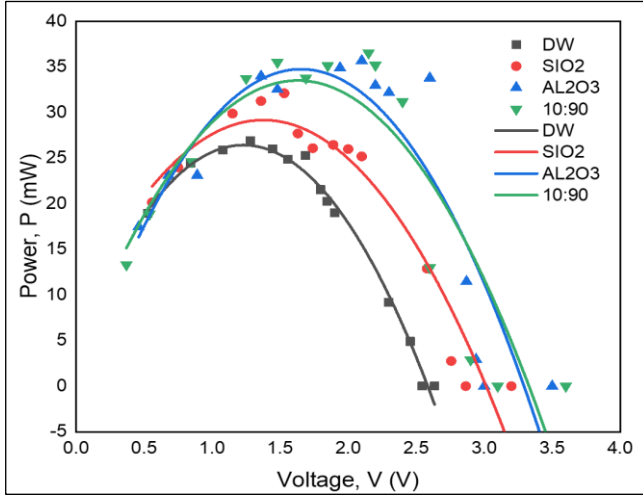


Figure 14: Power, *mW* against Voltage, *V* for all fluid

Conclusion

In this study, the effect of different cooling fluids on the PEMFC cooling plate integrated with TEG performances was discussed. The results of the experiment showed that hybrid nanofluids have increased the heat transfer performance of the cooling plate. This has resulted in the highest heat transfer coefficient by the hybrid nanofluids in PEMFC cooling applications. The improvement in heat transfer of the PEMFC cooling plate has resulted in a bigger temperature difference in TEG's hot and cold sides. The TEG performance also displayed that a hybrid nanofluid ratio of 10:90 obtained the highest power as compared to other cooling fluids. Thus, this study concludes that hybrid nanofluids can enhance the cooling plate's performance through better waste heat recovery. This is due to the improved thermal conductivity of hybrid nanofluids compared to base fluid. However, more thorough research on the hybrid nanofluids used as a coolant in the PEMFC needs to be further explored in the full stack of PEMFC to understand more about its mechanism for better performance in PEMFC and TEG integration.

Contributions of Authors

The authors confirm the equal contribution in each part of this work. All authors reviewed and approved the final version of this work.

Funding

The authors would like to thank the College Of Engineering, Universiti Teknologi MARA (UiTM) for the facilities and the financial support given under GIP - 600-RMC/GIP 5/3 (119/2023).

Conflict of Interests

All authors declare that they have no conflicts of interest.

Acknowledgment

The acknowledgment could go to those persons who provided intellectual assistance, technical help (including with writing, data analyses, proofreading, etc.), or specific equipment or materials.

References

- [1] Wilberforce, Tabbi, A. G. Olabi, Imran Muhammad, Abed Alaswad, Enas Taha Sayed, Ahmed G. Abo-Khalil, Hussein M Maghrabie, Khaled Elsaid, and Mohammad Ali Abdelkareem, "Recovery of waste heat from proton exchange membrane fuel cells – A review," *International Journal of Hydrogen Energy*, vol. 52, pp. 933-972, 2024. <https://doi.org/10.1016/j.ijhydene.2022.08.069>.
- [2] T. R. Ralph, "'Principles of Fuel Cells'," *Platinum Metals Review*, vol. 50, no. 4, pp. 200-201, 2006. <https://doi.org/10.1595/147106706X158789>.
- [3] Baroutaji, A., Arjunan, A., Ramadan, M., Robinson, J., Alaswad, A., Abdelkareem, M. A., & Olabi, A. G., "Advancements and prospects of thermal management and waste heat recovery of PEMFC," *International Journal of Thermofluids*, vol. 9, pp. 100064-100064, 2021. <https://doi.org/10.1016/j.ijft.2021.100064>.
- [4] H. Jouhara, N. Khordehgah, S. Almahmoud, B. Delpech, A. Chauhan, and S. A. Tassou, "Waste heat recovery technologies and applications," *Thermal Science and Engineering Progress*, vol. 6, pp. 268-289, 2018. <https://doi.org/10.1016/j.tsep.2018.04.017>.
- [5] M. Alam, K. Kumar, and V. Dutta, "Dynamic modeling and experimental analysis of waste heat recovery from the proton exchange membrane fuel cell using thermoelectric generator," *Thermal Science and Engineering*

- Progress*, vol. 19, pp. 100627-100627, 2020. <https://doi.org/10.1016/j.tsep.2020.100627>.
- [6] H. Jouhara, N. Khordehgah, S. Almahmoud, B. Delpech, A. Chauhan, and S. A. Tassou, "Thermoelectric generator (TEG) technologies and applications," *International Journal of Thermofluids*, vol. 9, pp. 100063-100063, 2021. <https://doi.org/10.1016/j.ijft.2021.100063>.
- [7] M. T. Børset, Ø. Wilhelmsen, S. Kjelstrup, and O. S. Burheim, "Exploring the potential for waste heat recovery during metal casting with thermoelectric generators: On-site experiments and mathematical modeling," *Energy*, vol. 118, pp. 865-875, 2017. <https://doi.org/10.1016/j.energy.2016.10.109>.
- [8] J.-H. Meng, X.-D. Wang, and W.-H. Chen, "Performance investigation and design optimization of a thermoelectric generator applied in automobile exhaust waste heat recovery," *Energy Conversion and Management*, vol. 120, pp. 71-80, 2016. <https://doi.org/10.1016/j.enconman.2016.04.080>.
- [9] J.-H. Meng, D.-Y. Gao, Y. Liu, K. Zhang, and G. Lu, "Heat transfer mechanism and structure design of phase change materials to improve thermoelectric device performance," *Energy*, vol. 245, pp. 123332-123332, 2022. <https://doi.org/10.1016/j.energy.2022.123332>.
- [10] A. Ramkumar and M. Ramakrishnan, "Performance improvement of thermoelectric generator by drooping the cool side temperature with thermacool 0.3M coating," *Case Studies in Thermal Engineering*, vol. 39, pp. 102418-102418, 2022. <https://doi.org/10.1016/j.csite.2022.102418>.
- [11] K. Karthick, S. Suresh, M. M. M. D. Hussain, H. M. Ali, and C. S. S. Kumar, "Evaluation of solar thermal system configurations for thermoelectric generator applications: A critical review," *Solar Energy*, vol. 188, pp. 111-142, 2019. <https://doi.org/10.1016/j.solener.2019.05.075>.
- [12] Ruan, H., Xie, H., Wang, J., Liao, J., Sun, L., Gao, M., & Li, C., "Numerical investigation and comparative analysis of nanofluid cooling enhancement for TEG and TEC systems," *Case Studies in Thermal Engineering*, vol. 27, pp. 101331-101331, 2021. <https://doi.org/10.1016/j.csite.2021.101331>.
- [13] N. Sezer, M. A. Atieh, and M. Koç, "A comprehensive review on synthesis, stability, thermophysical properties, and characterization of nanofluids," *Powder Technology*, vol. 344, pp. 404-431, 2019. <https://doi.org/10.1016/j.powtec.2018.12.016>.
- [14] R. S. Khedkar, S. S. Sonawane, and K. L. Wasewar, "Influence of CuO nanoparticles in enhancing the thermal conductivity of water and monoethylene glycol based nanofluids," *International Communications in Heat and Mass Transfer*, vol. 39, no. 5, pp. 665-669, 2012. <https://doi.org/10.1016/j.icheatmasstransfer.2012.03.012>.

- [15] A. M. Ajeena, P. Víg, and I. Farkas, "A comprehensive analysis of nanofluids and their practical applications for flat plate solar collectors: Fundamentals, thermophysical properties, stability, and difficulties," *Energy Reports*, vol. 8, pp. 4461-4490, 2022. <https://doi.org/10.1016/j.egy.2022.03.088>.
- [16] J. He, K. Li, L. Jia, Y. Zhu, H. Zhang, and J. Linghu, "Advances in the applications of thermoelectric generators," *Applied Thermal Engineering*, vol. 236, pp. 121813-121813, 2024. <https://doi.org/10.1016/j.applthermaleng.2023.121813>.
- [17] Abdelkareem, M. A., Mahmoud, M. S., Elsaid, K., Sayed, E. T., Wilberforce, T., Al-Murisi, M., & Olabi, A. G., "Prospects of Thermoelectric Generators with Nanofluid," *Thermal Science and Engineering Progress*, vol. 29, pp. 101207-101207, 2022. <https://doi.org/10.1016/j.tsep.2022.101207>.
- [18] D. R. Karana and R. R. Sahoo, "Effect on TEG performance for waste heat recovery of automobiles using MgO and ZnO nanofluid coolants," *Case Studies in Thermal Engineering*, vol. 12, pp. 358-364, 2018. <https://doi.org/10.1016/j.csite.2018.05.006>.
- [19] D. R. Karana and R. R. Sahoo, "Performance effect on the TEG system for waste heat recovery in automobiles using ZnO and SiO nanofluid coolants," *Heat Transfer—Asian Research*, vol. 48, no. 1, pp. 216-232, 2019. <https://doi.org/10.1002/htj.21379>.
- [20] S. Khalid, I. Zakaria, W. H. Azmi, and W. A. N. W. Mohamed, "Thermal–electrical–hydraulic properties of Al₂O₃–SiO₂ hybrid nanofluids for advanced PEM fuel cell thermal management," *Journal of Thermal Analysis and Calorimetry*, vol. 143, no. 2, pp. 1555-1567, 2021. <https://doi.org/10.1007/s10973-020-09695-8>.
- [21] D. Dhinesh Kumar and A. Valan Arasu, "A comprehensive review of preparation, characterization, properties and stability of hybrid nanofluids," *Renewable and Sustainable Energy Reviews*, vol. 81, pp. 1669-1689, 2018. <https://doi.org/10.1016/j.rser.2017.05.257>.
- [22] S. M. Vanaki, P. Ganesan, and H. A. Mohammed, "Numerical study of convective heat transfer of nanofluids: A review," *Renewable and Sustainable Energy Reviews*, vol. 54, pp. 1212-1239, 2016. <https://doi.org/10.1016/j.rser.2015.10.042>.
- [23] M. Borzuei and Z. Baniamerian, "Role of nanoparticles on critical heat flux in convective boiling of nanofluids: Nanoparticle sedimentation and Brownian motion," *International Journal of Heat and Mass Transfer*, vol. 150, pp. 119299-119299, 2020. <https://doi.org/10.1016/j.ijheatmasstransfer.2019.119299>.
- [24] R. Abu Bakar, B. Singh, M. F. Remeli, and O. K. Seng, "Experimental Electrical Characterisation of Thermoelectric Generator using Forced Convection Water Cooling," *Journal of Mechanical Engineering*, vol. 17, no. 1, pp. 1-16, 2020. <https://doi.org/10.24191/jmeche.v17i1.15215>.